http://www.zju.edu.cn/jzus; E-mail: jzus@zju.edu.cn
ISSN 1009 - 3095 *Journal of Zhejiang University SCIENCE* V.4, No.5, P.565 - 572, Sep. - Oct., 2003

Experimental study on centrifugal concrete-filled steel tubes under bending and torsion*

JIN Wei-liang(金伟良)†[1], QU Chen(曲晨)[2], YU Yi(于弋)[1]

([1] *Department of Civil Engineering, Zhejiang University, Hangzhou 310027, China*)

([2] *Department of Civil Engineering, Zhejiang University of Science and Technology, Hangzhou 310012, China*)

†E-mail: jinwl@civil.zju.edu.cn

Received Sept.10, 2002; revision accepted Jan.6, 2003

Abstract: A real-size experiment on 11 tubes was done to study the performance of centrifugal concrete-filled steel tubes under bending and torsion. This paper first introduces the relevant operating method, equipment, subjects and processes. The factors that affect deformation and stiffness and the break mechanism under different loading were studied. Experimental stress analysis showed that the values of practical critical stress of steel tubes accorded well with the MISES Yielding Rule. The correlative equation (on the bearing capacity of a structural member under bending and torsion) deduced in this study may provide valuable reference for the design of this structural member.

Key words: Centrifugal concrete-filled steel tube, Bending and torsion, Stiffness, Distortion, Bearing capacity

Document code: A **CLC number:** TU375

INTRODUCTION

Concrete-filled steel tubes are now widely used in factories, power stations, bridges, etc. Centrifugal concrete-filled steel tubes are hollow structural members centrifugated by high-speed centrifuge, and are therefore of considerably less weight than traditional tubes. As they are formed on centrifuge, centrifugal concrete-filled steel tubes have advantages of relatively better maintenance, more close-grained concrete filling, and obviously improved strength, especially improved compression strength. In actual practice, there are always combinations of different loads on a structural member. Bending and torsion is one of these combinations. Most researches on centrifugal concrete-filled steel tubes focused on the performance of such a structural member under single load (Xu *et al.*, 1991; Ge, 1987; Song, 1988; National Electric Power Ministry, 1996; Fu, 2000; Jin *et al.*, 2001a); none on the performance under bending and torsion. Therefore to carry out studies on centrifugal concrete-filled steel tubes under bending and torsion is of great value for popularizing application of this structure. Real-size experiments were carried out to study the performance and mechanism of this structural member under different loading conditions (varied M/T, Figs.1 - 3). The correlative equation (on the bearing capacity of this structural member under bending and torsion) deduced in this study can serve as valuable reference for application of such structures.

TEST PROGRAM

1. Specimens

Because there is no national criterion on the mechanical capabilities of centrifugal concrete filled steel tubes yet, aside from the strength of standard cubic concrete specimen, the strength, elastic modulus and Poisson ratio of the centrifugal concrete tubes were measured to obtain the relevant mechanical parameters of the materials. Test data on the compression strength are shown in Table 1 and Table 2.

* Project supported by the Zhejiang Province Electric Power Designing Institute and the Electric Power Ministry of China

Table 1 Test data for the centrifugal concrete tubes

Specimens	D(mm)	L(mm)	t(mm)	A(mm^2)	P_u(kN)	f_{cu}(MPa)	E_c($\times 10^4$MPa)
# 1	200	200	21.75	12180	490	40.3	3.83
# 2	200	200	20.25	11933	460	38.5	3.69
# 3	200	200	20.50	11560	496	42.9	4.53
# 4	200	200	21.75	12180	380	31.2	3.81
# 5	200	200	19.80	11209	334	29.8	3.72
# 6	200	200	20.50	11560	454	39.3	4.12

* Note: D = external diameter; L = length of tube; t = thickness of tube wall; A = contact area; P_u = ultimate pressure; f_{cu} = ultimate compressive strength of concrete; E_c = elastic modulus of concrete.

Table 2 Test data for the outer steel

Specimens	L(mm)	b(mm)	t(mm)	T_u(kN)	σ_b(MPa)	σ_u(MPa)	σ_b/σ_u
# 1	343	31.7	4.37	44.5	264	305	0.866
# 2	342	32.2	4.96	44.5	275	300	0.917
# 3	365	31.5	4.92	40.5	270	302	0.894
# 4	365	31.35	2.95	20.5	200	250	0.800
# 5	350	31.1	3.02	21.0	204	254	0.803
# 6	375	32.3	3.04	20.0	195	248	0.786

* Note: L = length of specimen; b = breadth of specimen; T_u = ultimate torsion force σ_b = yield stress of steel; σ_u = ultimate stress of steel

2. Parameters of the specimens

Specifications for the specimens: The external diameter of the steel tubes (D) was 200 mm. The thickness of steel tubes (t_s) varied from 3 mm to 5 mm. The thickness of the concrete tubes (t_c) varied from 20 mm and 30 mm.

Numbers of the specimens: There were altogether 4 types of 11 specimens with different length-diameter ratios ($L/D = \lambda = 10, 15$; L, length), steel-concrete ratios (S/C)(S, areas of steel section and C, areas of concrete) and vacancy ratios(V). The main parameters for the specimens are shown in Table 3.

Table 3 Main parameters for the specimens

Specimens	D(mm)	t_s(mm)	t_c(mm)	L(mm)	L/D	S/C	V
# 1	200	3	20	3000	15	0.17	0.794
# 2	200	3	20	3000	15	0.17	0.794
# 3	200	3	20	3000	15	0.17	0.794
# 4	200	5	25	3000	15	0.236	0.737
# 5	200	5	25	3000	15	0.236	0.737
# 6	200	3	25	2000	10	0.14	0.742
# 7	200	3	25	2000	10	0.14	0.742
# 8	200	3	25	2000	10	0.14	0.742
# 9	200	5	25	2000	10	0.236	0.737
# 10	200	5	25	2000	10	0.236	0.737
# 11	200	5	25	2000	10	0.236	0.737

3. Application of load and test procedures

The tests were done by using the appropriate torsion machine in the structure laboratory of Zhejiang University. Fig. 1 shows the whole set of equipments and the application of load. Its advantage is that some tests of large specimens can performed by the machine, so as to avoid error caused by the size effect. On each end of the

specimens is a pulley connected with the fan-shaped board through which pulling force may be transferred into twisting force uniformly. A force sensor mounted in a section of the steel cable recorded the pulling force. Two ways were used to exert bending load force. One way was to set a jack on the medium port of the specimen. The other was to set a jack on each trisection of the specimen(Jin *et al*., 2001b). The value of the bending force can be shown on the pressure gauge connected to the jack oil pump.

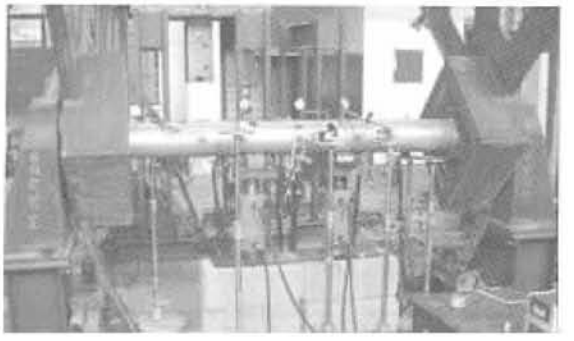

Fig.1 Equipment and the application of load

The loading process was in steps. The torsion was graded by tenths of the estimated ultimate torsion. After yielding, each incremental change was reduced to twentieth, to fortieth, etc. of the estimated ultimate torsion. The bending force kept increasing by tenths of the estimated ultimate bending force all along the specimen. To make clear the mechanical property of the specimen, a load-unload cycling method was used. To minimize error arising from occlusion and friction of the parts of the machine, after each unloading, a tiny portion of load was kept and five minutes after loading, the meter data were recorded.

4. Measurement of distortion and strain

The observations were mainly on the strain of the steel tube, angular displacement and radial distortion. On the exterior of one specimen there were altogether 24 strain-measured points that distributed respectively on the ends, quarters and section. There were eight points on the section and four on each other section. On each point a right-angle strain-gauging slice was set. YJ-22 Static Strain Recording Instruments were used to record the strains. The circuitry connection was half-bridge connection with twenty points shared temperature compensation. A clock dial was set at each end of the twisting machine's spin axis to indicate the twisting angle of the specimen. Another method applied in the meantime was to attach a piece of coordinate paper around the circumference of each end of the specimen. The recorded circular displacement of the gauged spot then could be converted into the twisting angle of the specimen. As the result showed, the data obtained from the second method are more precise than those from the first one; mainly because the second method avoided the errors arising from occlusion and friction of the spin axis.

The centigrade displacement gauges with measuring range from 0 mm to 3 mm were set at the five sections mentioned above to gauge the radial displacements of different sections of the specimen. The experimental curve of the relationship between torsion and shearing strain under different moments is shown in Fig.2.

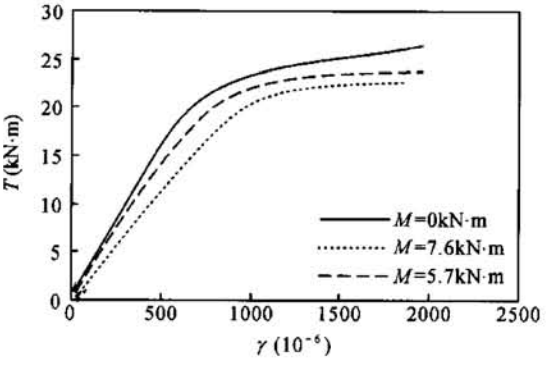

Fig. 2 Relationship between torsion and shearing strain under different moments

RESULTS AND DISCUSSION

1. Analysis of the test results

Tests under different loading conditions showed that with a constant moment, the relationship between torsion and angular displacement consisted of three phases: elastic, elastic-plastic and ultimate. In the case A, pure torsional moment ($M = 0$) was applied before the yield value. But with the increase of bending moments, the yielding load and ultimate load decreased. Especially during the plastic phase,

softening phenomenon might occur with considerable bending moments. Although the bending moment on the specimen had little effect on the torsion stiffness in the elastic phase, in elastic-plastic and succeeding phases, the torsion stiffness decreased greatly with the increase of the bending moments as shown in Fig.3.

It is obvious in Fig.4 that the torsion on the specimen had little effect on the radial displacement(f) in the elastic phase. In the elastic-plastic phase, with a constant bending moment, the radial displacement increased sharply while the torsion increased with increasing bending moment; the resulting torsion for the same radial displacement decreased evidently. And if the bending moment increased to some extent, the resulting torsion decreased sharply and softening might occur.

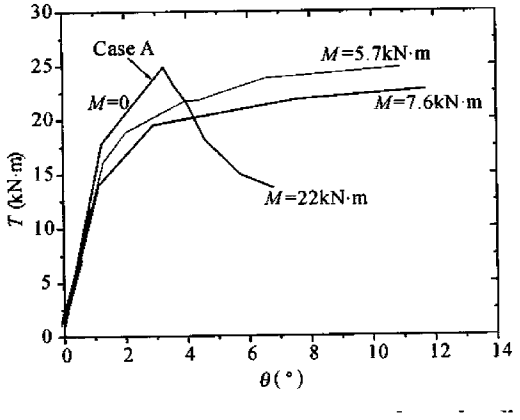

Fig.3 Relationship between torsion and angular displacement with different moments

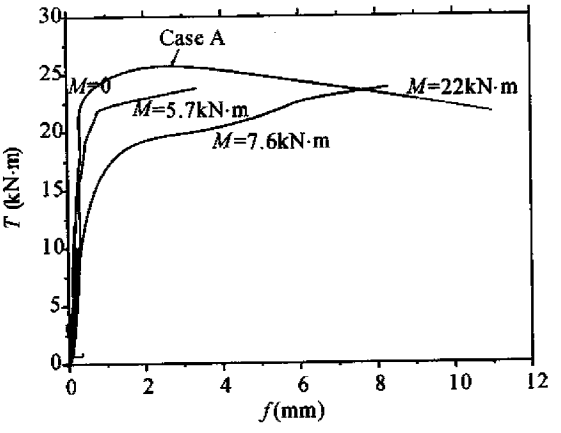

Fig.4 Relationship between torsion and bending deflection with different moments

2. Analysis of the bending and torsion mechanism of centrifugal concrete filled steel tube

It was clear that the mechanical performance of the specimens was desirable in the elastic phase. But when micro cracks appeared during the plastic phase, the bond between the concrete and the steel tube broke partially with the constant increase of the outer load. In addition, due to the original bug (the initial errors in the making) on the specimen, the outer steel tube tended to warp when the torsion increased. All these resulted in decreased bearing capacity of the specimen. By analysis, the mechanism involved:

(1) The brace of the inner concrete tube helped the steel tube during the elastic phase to overcome the tendency to warp because of partial defects of the specimen. Therefore, the specimen will not warp partially in both elastic and elastic-plastic phases. In ultimate phase, the steel tube may warp partially because of the breakup of the inner concrete. In this way, the outer steel may exert its full strength.

(2) Due to the hoop effect of the outer steel tube, the specimen showed remarkable shearing resistance. Fig.5 and Table.4 illustrate the torsion distributed over the steel and concrete when a specimen of 5 mm length steel tube is under torsion. In the general, without the outer hoop effect, the shear failure of the concrete tube is brittle failure.

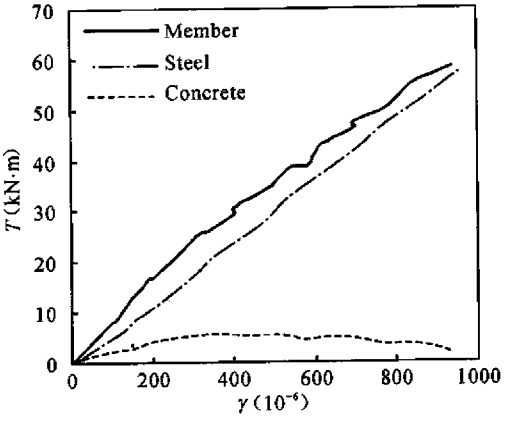

Fig.5 Torsion shared by steel and concrete

Table 4 Torsion distributed over on concrete tube

Order	Total torsion T(kN·m)	Torsion on steel T_s(kN·m)	Torsion on concrete T_c(kN·m)	T_c/T
1	0	0	0	
2	8.036377	6.3092	1.7272	0.2149
3	16.94062	12.133	4.8076	0.2838
4	24.43887	18.442	5.9966	0.2454
5	30.52731	24.266	6.2612	0.2051
6	35.06112	30.09	4.9712	0.1418
7	38.74665	33.245	5.5021	0.1420
8	42.29196	37.006	5.2862	0.1250
9	43.42678	38.462	4.9650	0.1143
10	46.69023	42.466	4.2245	0.0905
11	50.80683	47.562	3.2453	0.0639
12	54.64133	50.716	3.9252	0.0718
13	58.33548	57.025	1.3101	0.0225

It is evident in Fig.5 that with the restraint of the outer steel tube, after the shearing stress of the concrete maximizes, the bearing capacity will not decrease; instead, the tensile stress is gradually shared by the steel tube while the concrete with minor cracks continue to partially bear the tensile stress, and therefore ensure the maximum bearing resistance of the concrete as the specimen is under torsion. The qualitative change occurs when the torsion failure of the specimen and the brittle failure of the concrete tube are transformed into plastic failure.

(3) Like compressed structures, the centrifugal concrete filled steel tube showed elasticity in usual use and plasticity in the breaking process. The thickness of the inner concrete tube wall has great effect on the ultimate strength and plastic distortion capacity of the structure. The shearing stress equation $\tau_x = r(T/J_p)$ (J_p is the equivalent polar second-area moment of the cross section) and the normal stress equation $\sigma_x = r(M/J_z)$ (J_z is the second-area moment of the cross section relative to the bending z axis) showed that the radius of the concrete is approximate to that of the outer steel tube. As a result, the inner part of the concrete tube whose stress is relatively large will soon reach its failure strength. On the contrary, a thicker wall means smaller stress on the inner concrete. The outer part of the concrete tube is restrained simultaneously by the inner part of the concrete tube and the steel tube, and is therefore in a triaxial state of compression. As a result, the bearing capacity will not decline sharply. This case is similar to that of a solid concrete filled steel tube. As analyzed from the test data, for specimen under maximum load, the stress on the outer part of the steel tube in the dangerous section accord with Mises rules. This demonstrates that the binding force between the concrete and the steel tube is outstanding. As far as the bearing capacity of the steel tube is concerned, with a smaller thickness of the concrete tube, the plastic distortion phase is relatively short, and ultimate failure occurs comparatively fast. While with a larger thickness of the concrete tube, the case is similar to that of solid concrete filled steel tube.

(4) There are mainly two failure modes of the specimen under bending and torsion. The first type is that torsion is the dominant load. Spiral diagonal cracks appear on the inner part of the concrete under shearing stress. So the concrete is divided into compressed ribs to share the compressive stress component of shearing stress. In the biggest moment section, the tensile stress together with the compressive stress may break the local concrete and then torsion failure will occur on this section. On the contrary, when bending is the dominant load, transverse cracks appear first in the biggest moment section due to the bending tensile stress. So compressed concrete ribs are not likely to form and consequently the local steel has to share more stress. When the local load reaches the ultimate bearing capacity, bending failure will occur. Fig.6 shows

the failure inside the concrete when the specimen is essentially under torsion failure and Fig. 7 show the failure modes in torsion and bending.

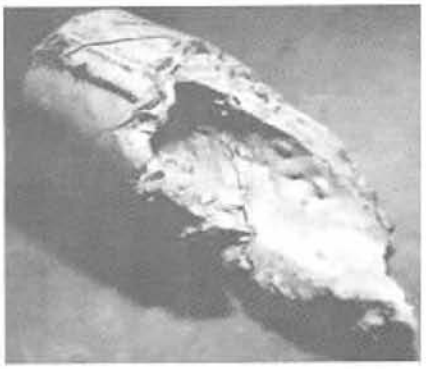

Fig.6 Failure of the inside concrete

Fig.7 The failure modes in torsion and bending

COMBINED STRESSES OF CRITICAL SECTIONS

The following is the Mises Yielding Equation (Zhuang *et al*., 1984):

$$(\sigma_x - \sigma_y)^2 + (\sigma_y - \sigma_z)^2 + (\sigma_z - \sigma_x)^2 + 6(\tau_{xy}^2 + \tau_{yz}^2 + \tau_{zx}^2) = 2\sigma_s^2 \quad (1)$$

In this test, the strain of the outer steel tube can be approximately deemed as plane strain. So the following equation is applicable:

$$\sigma_z = \frac{1}{2}(\sigma_x + \sigma_y);\ \tau_{zx} = \tau_{zy} = 0. \quad (2)$$

Then the Mises Equation in this test can be deduced as

$$(\sigma_x - \sigma_y)^2 + 4\tau_{xy}^2 = \frac{4}{3}\sigma_s^2. \quad (3)$$

From the equations above the relation between $(\sigma_x - \sigma_y)/\sigma_s$ and τ_{xy}/σ_s is obtained as shown in Fig. 8. It is obvious that the ultimate combined stresses of the specimen accord well with the Mises Yielding Rule and are almost not subject to the relevant parameters and loading conditions.

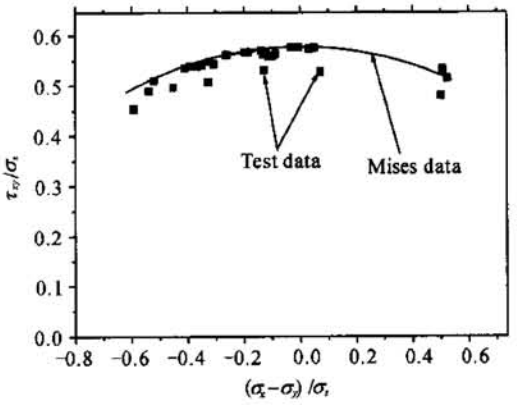

Fig.8 Comparison of test Mises stresses and theoretical Mises stress

In Table 5 the ratio of Mises stress deduced from the test to that of theoretical deduction with different loading conditions is listed.

Table 5 Test Mises stress versus theoretical Mises stress

M/T (thickness of steel tube)	Test average (MPa)	Test mean-square deviation (MPa)	Theoretical data (MPa)	Test data/Theoretical data
2/3(3mm)	267.372	8.709	288.675	0.926
1/1(3mm)	282.215	4.767	288.675	0.978
3/2(3mm)	286.670	2.165	288.675	0.993
1/4(5mm)	326.654	12.147	346.410	0.943
1/3(5mm)	338.722	6.717	346.410	0.978
1/2(5mm)	341.637	4.297	346.410	0.986

* Note: M = test bending force; T = test torsion force.

The following is the shearing strain (γ_{xy}) equation of the outer part of the steel tube ε_x, ε_y, ε_{45} are the readings of the three-element rectangular rosette strain gauge mounted on the steel part.

$$\gamma_{xy} = \varepsilon_x + \varepsilon_y - 2\varepsilon_{45} \tag{4}$$

Once ε_x, ε_y, γ_{xy} were known, the stress-strain relations of the steel part could be used to determine the stresses σ_x, σ_y and τ_{xy}, and the tested Mises stress values (σ_e^M) came from the equation:

$$\sigma_e^M = [(\sigma_x - \sigma_y)^2 + 4\tau_{xy}^2]^{0.5} \tag{5}$$

The theoretical Mises stress values (σ_t^M) came from the equation:

$$\sigma_t^M = (4\sigma_b^2/3)^{0.5} \tag{6}$$

The yield stress (σ_b) of steel tube is shown in Table 2. Table 5 shows that when the specimen broke, the stress of the steel tube in the critical section reached the ultimate stress of the steel; indicating that the steel and the concrete in the structure had exerted their maximum strength.

CORRELATION EQUATION ON BEARING CAPACITY UNDER BENDING AND TORSION

The data on warp failure of ribbed tubes under combination of bending and torsion are limited to the test data that Galcit (Anon, 1943) got; from which a correlation equation on normal stress and shearing stress of isotropic tubes could be deduced. It is an ellipse equation (Gerard *et al.*, 1957):

$$\left(\frac{\sigma}{\sigma_0}\right) + \left(\frac{\tau}{\tau_0}\right)^2 = 1 \tag{7}$$

But when Galcit applied this equation to analyze test data, it was found that they were greatly dispersed along an elliptical curve between a parabola and a circle. Consistent data on the dispersal are not available. The relationship of the test data may be shown by a function involving M/M_u and T/T_u.

A test analysis of the centrifugal concrete filled steel tube specimens under bending and torsion with different loading conditions was done. Finite element methods could be used to calculate the bearing capacity of structures under bending and torsion, but that will be too complex and not easy to be applied to practical problems. Therefore, a simplified formula for the bearing capacity must be used.

The tests based the shapes of the correlation equation curves of centrifugal concrete filled steel tube specimens were similar even under different loading conditions. So the above model of M and T can be adopted. On assumption that the correlation curve of a specimen is between a parabola and a circle (Anon, 1943), according to the test result, the correlation curve (Fig. 9) can be expressed by the following formula:

$$\left(\frac{M}{M_u}\right)^{1.9} + \left(\frac{T}{T_u}\right)^2 = 1 \tag{8}$$

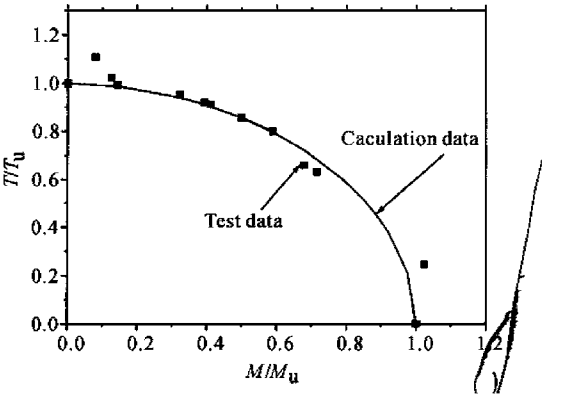

Fig. 9 Relationship between (M/M_u) and (T/T_u)

M_u and T_u are respectively the ultimate moment and ultimate torsion under a single load. T_u is the tested value of the specimens under torsion (Fu, 2000). M_u was deduced from the structural design criterion of the National Electric Power Ministry, which is Technical Code on centrifugal concrete-filled thin-wall steel tubular structure. $M_u = \frac{\phi}{1 + 1.55\phi} N_0 r$ (National Electric Power Ministry, 1996); $N_0 = A_s f_s + 1.3 A_c f_c$ (National Electric Power Ministry, 1996) is the design value of the ultimate bearing capacity of a compressed short column. ϕ is the steel percentage eigenvalue of the structure. $\phi = \frac{A_s f_s}{1.3 A_c f_c}$ (National Electric Power Ministry, 1996); r is the external radius of the outer steel tube.

CONCLUSIONS

The relationship between distortion and load of centrifugal concrete filled steel tubes with different loading conditions can be divided into three phases: elastic distortion, elastic-plastic distortion and ultimate distortion. In the elastic distortion phase, steel works together with concrete. In the elastic-plastic distortion phase, cracks appear inside the concrete which loses tensile strength gradually. The short diagonal concrete bars serve as reinforced ribs. In the ultimate phase, the plastic distortion of steel exceeds that of concrete. The concrete is subjected to ultimate compression stress and the local steel tube loses its limitation function and local warping failure occurs. There are mainly two types of ultimate failure: torsion failure and bending failure. Generally those failures are plastic. But when the wall of the steel tube is too thin or machining defects exist in the tube, some forms of fragile failure such as losing stability or weld breaking may occur.

Considering the test errors and original defects on the specimen, the Mises stress is almost not subject to the ratio of bending versus torsion. It means that with different loading conditions, the complex stress on the critical section reaches the Mises stress ultimately. The relationship between bending moments and torsion can be expressed by an elliptical curve that is a cross between a circle and a parabola. The length-diameter ratio (L/D) influences the distortion of the structure to some extent and its influence on the ultimate bearing capacity is considerable.

The bearing capacity of the newly-developed structural member, centrifugal concrete filled thin-wall steel tube under compound load of bending and torsion was studied in this work whose result provide valuable reference for practical application.

References

Anon, 1943. Some Investigations of the General Instability of Stiffened Metal Cylinders. VII – Stiffened Metal Cylinders Subjected to Combined Bending and Torsion. NACA TN 911, 1943.

Fu, J., 2000. Test Research of Bearing Torsion Capacity of Centrifugal Concrete filled Thin-Wall Steel Tubular Structure. Thesis for Master Degree in Zhejing University(in Chinese).

Ge, Z.G., 1987. Strength Testing Technology and Mechanical Performance of Centrifugal Concrete. Zhejiang province Electric Power Design Institute papers(in Chinese).

Gerard, G. and Becker, H., 1957. Handbook of Structural Stability. Part III – Buckling of Curved Plates and Shells. NACA TN 3783.

Jin, W.L., Ge, Z.G. and Qu, C., 2001a. Test Research of Bearing Torsion capacity of centrifugal concrete filled thin-wall steel tubular structure. Chinese Steel-Concrete Composite Conference eighth academic meeting papers (in Chinese).

Jin, W.L. and Zhao, Y.X., 2001b. Effect of corrosion on bond behavior and bending strength of reinforced concrete beams. *Journal of Zhejiang University SCIENCE*, **2**(3):298 – 308.

National Electric Power Ministry, 1996. Technical Code on the Centrifugal Concrete filled Thin-Wall Steel Tubular Structure(DL/T 5030-1996). Chinese National Electric Power Ministry(in Chinese).

Song, Y.L., 1988. Strength Research on Centrifugal Concrete Steel Tubular Column. Thesis for Master's Degree in Zhejing University(in Chinese).

Xu, G.L. and Ge, Z.G., 1991. Centrifugal Concrete Filled Thin-wall Steel Tubular Structure. Zhejiang province Electric Power Design Institute papers(in Chinese).

Zhuang, L.N., Ma, X.S. and Jiang, L., 1984. Engineering Plastic Mechanics. Chinese Advanced Education Publisher, Beijing(in Chinese).